CHINESE OPTICS LETTERS

Vol. 21, No. 4 | April 2023

Smith–Purcell radiation-like photoacoustic phased array

Dongyi Shen (沈冬屹)[1], Guolin Zhao (赵国林)[1], Xianfeng Chen (陈险峰)[1], and Wenjie Wan (万文杰)[1,2*]

[1] School of Physics and Astronomy, Shanghai Jiao Tong University, Shanghai 200240, China

[2] University of Michigan-Shanghai Jiao Tong University Joint Institute, Shanghai Jiao Tong University, Shanghai 200240, China

*Corresponding author: wenjie.wan@sjtu.edu.cn

Received November 15, 2022 | Accepted January 3, 2023 | Posted Online March 14, 2023

Relativistic electrons moving over a periodic metal grating can lead to an intriguing emission of light, known as Smith–Purcell radiation (SPR), the precursor of the free-electron laser. The speed of light plays a critical role in the far-field emission spectrum. Inspired by this photonic SPR, here we experimentally demonstrate a photoacoustic phased array using laser-induced shock waves. We observe acoustic radiation spectrum in the far field, perfectly predicted by a universal theory for the SPR. This scheme provides a tool to control the acoustic radiation in the near field, paving the way toward coherent acoustic wave generation and microstructure metrology.

Keywords: nonlinear optics; Smith–Purcell radiation; laser-induced shock wave; photoacoustic phased array.
DOI: 10.3788/COL202321.041901

1. Introduction

Smith–Purcell radiation (SPR), a classical type of electromagnetic radiation generated from free electrons moving over a metallic grating[1], allows broadband emission of electromagnetic (EM) waves ranging from terahertz waves, visible light to X-ray[2–4], building up the foundation for the free-electron laser[5,6], which is capable of producing high-intensity coherent and broadband sources as electron microbunches travel through designed magnetic undulators in a similar manner[7]. Compared with other relativistic radiation sources such as synchrotron and cyclotron radiation[8,9], SPR-based free-electron light sources are more compact and tunable, given the fact that the wavelength of the emitted light depends on the energy of the electron beam as well as the structure of the periodic surroundings. This offers an opportunity to further shrink the size of these devices with the help of the recent development of nanofabrication technologies, making it even possible to realize on-chip implements of such SPR-based light sources[10–13].

When electron wave packages travel near a metallic grating, SPR is generated and belongs to a thresholdless process, behaving like a simple Bragg scattering of the evanescent waves carried along with the electrons, where a constant light velocity fundamentally defines the angle relations of radiation's wavelength[14–17]. The speed of light directly determines the relative phase of scattering waves between two adjacent grating scatters. In a similar manner, a phased array, the emitters/scatters of a phase-controlled array, in microwaves[18,19], acoustics[20–22], and optics[23,24] can alter the emission angles by adjusting the relative phases in the array. The phase control can be easily implemented in the phased array case at each active emitter, while in the SPR case, the relative phases between two adjacent scatters are purely determined by the speed of light. It is interesting to explore analogous forms of SPR in other physical systems[25,26] like acoustics[27], phononics[28,29] and exciton-polariton[30], where the required excitation speed is more feasible compared to the photonic case. For example, a sharp shock wavefront can be analogously treated as an ultrabroadband acoustic wave source, imitating the moving free electron in the case of SPR.

In this work, we experimentally demonstrate a photoacoustic phased array with sequential laser-induced shock waves. The formed periodical grating results in a tunable acoustic radiation in the far field, where the radiation pattern exhibits an angular dispersion relation exactly like the SPR in the photonic case. Similar to its photonic counterpart, the observed photoacoustic phased array also depends on the effective moving velocity of excitation. These results connect the acoustic phased array to the concept of the Smith–Purcell effect, paving a new way for their practical application in microstructure sensing and coherent acoustic wave sources.

2. Methods

A classical SPR in photonics arises from the Bragg-type scattering of an electron wave package that is uniformly moving near a metal periodic grating. The electron can be considered as a single point source in time composed of ultrabroadband electromagnetic (EM) waves, which can be scattered into free space by each tooth on the grating. The scattered EM waves at a particular angle in the far field can be defined in their frequency/wavelength by the Bragg condition[15,17], where both the velocity of the moving electrons and the periodicity of the

grating play a prominent role in the angular emission spectrum. Ideally, a sharp acoustic wavefront, e.g., shock wave, travels uniformly at a speed of v near the top surface of a grating structure with a periodicity of D. Each tooth of the grating, as a point emitter, sequentially scatters the acoustic wave, forming an acoustic SPR. However, due to the limited propagation length of shock waves, we have to degrade such an analogy to photonic SPR and consider a sequentially excited phased array in Fig. 1, where each emitter can be successively ignited in time by laser-induced shock waves[21,22]. In this manner, each emitter mimics the scattering tooth in the SPR case, and the temporal delays between two adjacent emitters relate to the effective "moving" speed of an acoustic wavefront traveling on top. The temporal photoacoustic phased array emits different frequency waves, depending on the angular relationship as shown in Fig. 1(b), given the almost constant sound speed. Similar photoacoustic phased arrays have also been studied before but mainly on their phase-controlled emission patterns[21,22].

Due to the coherent constructions of wavefronts according to Huygens' principle shown in Fig. 1(b), such an SPR-like photoacoustic phased array emits its frequency-dependent radiation in different angles, like its counterpart in the photonic case. Inspired by the photonic SPR, we can obtain a universal angular relation for the constant sound speed as

$$m\lambda = v_a \cdot \Delta t = D \cdot \left(\frac{v_a}{v} - \cos\theta\right), \qquad m = 1, \qquad (1)$$

where D denotes the periodicity of such photoacoustic phased array emitters. v is the effective moving speed mentioned above, indicating a uniform time-sequentially excited phased array. v_a is the propagating velocity of the acoustic sound wave. θ is the emission angle shown in Fig. 1(b). This formula also resembles the photonic SPR case[2–4].

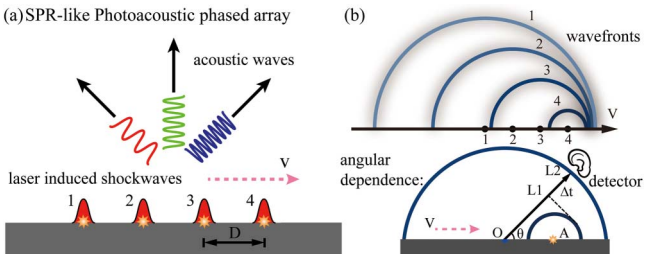

Fig. 1. Schematic of SPR-like photoacoustic phased array in a degraded form. (a) SPR-like photoacoustic phased array in a degraded form; the sequentially (1→4) excited laser-shock array emits acoustic radiation into the far field. (b) Upper, the resultant multiple propagating wavefronts from the procedure in (a); integers 1→4 denote each source and every wavefront in time sequence (indicated by the color). Lower, the effective quasi-phase line (dashed, normal to OL1 and OL2) depicts the angle dependence in the broadband SPR-like pattern in (b). By the moment when the detector captures the first shock front (blue) from source O, the secondary shock front from source A propagates to the detector. The delay time (Δt) for the detector to catch the later shock wave varies with the detection angle; accordingly, the received frequency is also changed.

3. Experiments and Results

Figure 2 shows the experimental realization of the photoacoustic phased array. A nanosecond laser (~10 ns, 200 μJ, 10 kHz) uniformly scans across a flat metallic surface to induce an array of plasma sparks at its focus via an f-θ lens. These sparks not only radiate bright visible light emission in Fig. 2(b) but also excite localized shock waves sequentially[31]. Note that the plasma sparks are not ignited at the same time; the time lag between two adjacent spots is determined by the laser repetition rate. To simulate the moving dynamics, a mirror is carefully mounted on a rotating motor and controlled by the voltage exerted. Thus, the mirror scanning speed and the constant repetition rate of the laser ensure equal distances between two adjacent sparks [Fig. 2(a)], such that the grating period is determined by $D = v/f_r$, where f_r is the repetition rate of the laser, v is the effective moving velocity of the laser spot, which is smaller than the sound speed. In this manner, we expect the same radiation pattern as proposed in Eq. (1). To measure the angular emission pattern, we place a microphone detector on a rotational stage. The microphone is connected to an oscilloscope to trace the received temporal acoustic signals [Fig. 2(c)] and their corresponding frequency spectra [Fig. 2(d)]. The laser output per pulse is around 0.2–0.3 mJ, with fluence of about ~10^1 J/cm^2, sufficient for laser-plasma (ablation) generation. Effectively, this configuration is similar to prior works of acoustic phased

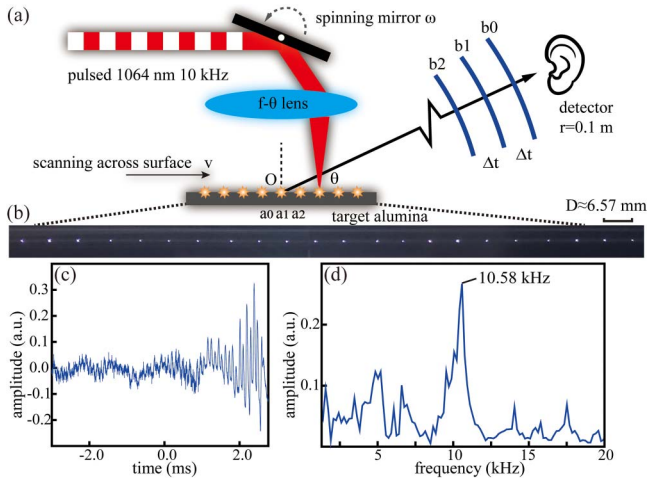

Fig. 2. Experimental observation of SPR-like photoacoustic radiation from a linear phased array in the far field. (a) Given a rotating mirror with a stable angular speed ω, the pump is scanned and focused onto the target alumina plate sequentially in the order a0→a1→a2, forming an effective laser-induced plasma shock wave phased array. The detector is placed r = 0.1 m from the array center O. The detector acquires the SPR signals also in the order b0→b1→b2. For a fixed detection angle θ and rotating ω, the time delay Δt remains unchanged and irrelevant to the detector's distance in the far field. (b) Snapshot of such an SPR-like linear phased array by laser-induced plasma; the periodicity D is about 6.57 mm. (c) Measured real-time temporal signal and (d) its corresponding spectrum with a peak frequency at 10.58 kHz. The signal is collected and processed at a surface scanning speed of 10 m/s (effective periodicity ~1 mm) at θ = 0°.

array[21,22]; however, the relative phase delays in their case were kept small enough only to tune the emission angle. In contrast, the large grating period in the current work well separates any two adjacent laser sparks so that the frequency spectrum in the far field can be studied.

Furthermore, by varying the detection angle θ and the moving velocity v, the far-field emission can be measured in terms of its peak frequency according to Eq. (1). As shown in Figs. 3(a)–3(d), for a fixed angle, the detected signal's frequency increases with the effective moving velocity of laser spots for two detection angles at 0° and 30°, fitting well with the theoretical curve calculated by Eq. (1). Note that the laser repetition rate is fixed at 10 kHz for both cases; the received signal can even double to twice the harmonic, ~20 kHz, in the forward direction (0°). Meanwhile, a full angle scan [Figs. 3(c) and 3(d)] reveals a declining trend of the signal's central frequency from the forward direction to the backward one (180°). This also coincides with the theoretical prediction. These results resemble the feature of the angular spectrum observed in photonic SPR[2–4], verifying similar radiation patterns for both cases.

Following the original SPR formulism in the photonic case, Eq. (1) only indicates the ideal theoretical results of the dispersive angle relation for estimating the central frequency. However, given the limited number of scatters in the current acoustic case, to fully understand the radiation spectra as shown in Figs. 3(a) and 3(b), we have to incorporate the radiation theory[32] by considering the limited array length, source spacing, induced phase item, and limited detection range. A directivity function (D_{array}) solving the above concerns then goes,

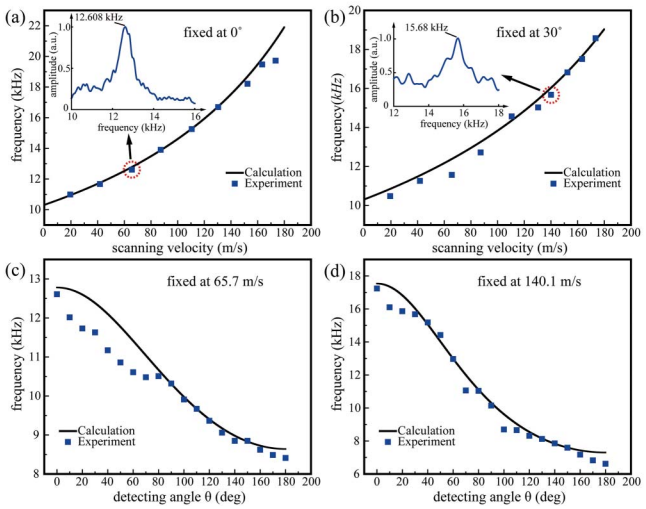

Fig. 3. Angular and velocity dependence of the phased array emission in the far field. (a) and (b) testify to the velocity-dependent frequency with fixed detection angles 0° and 30°, respectively. Insets in (a) and (b) are the spectrum collected under the condition with surface velocity 65.7 m/s (effective grating period 6.57 mm) and 140.1 m/s (effective grating period 14.01 mm). (c) and (d) demonstrate the angular dependence in the photoacoustic SPR specially picked at surface velocities of 65.7 m/s and 140.1 m/s. The dots are experimental measurements, and the solid lines are the theoretical curves calculated by Eq. (1).

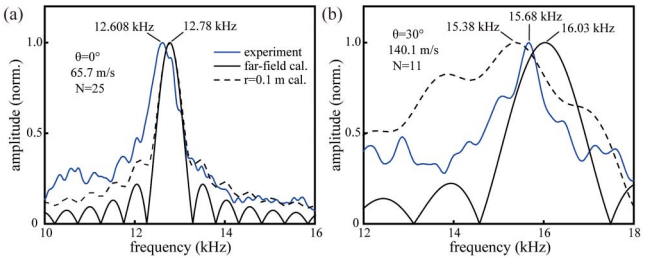

Fig. 4. Experimental (solid blue) and theoretical (black) radiation spectra at (a) $\theta = 0°$ and (b) $\theta = 30°$; (a) $N = 25$ (number of acoustic sources on the target), v_s = 65.7 m/s, $\theta = 0°$; (b) $N = 11$, v_s = 140.1 m/s, $\theta = 30°$. The directly detected temporal signals are averaged 128 times before fast Fourier transform (FFT) processing into experimental data via an oscilloscope. Note that the dashed black curves ($r = 0.1$ m) are calculated by directly summing up all the phase-delayed acoustic sources and gathering radiated acoustic pressure amplitude at given conditions. The detection angle θ for $r = 0.1$ m calculation is defined from the center of the array.

$$D_{\text{array}} = \left| \frac{\sin N\phi}{N \cdot \sin \phi} \right|, \tag{2}$$

where N is the number of the sources and the related phase item $2\phi = k \cdot D \cos\theta - k \cdot v_a \cdot \Delta T$ indicates that the acoustic pressure signals at distance r are relying on its spacing D and observation angle θ, which together compose the first term right of 2ϕ. As to the second term, it represents the inherent delay brought by time delay ΔT for the neighboring sources. In our scheme, the time delay is the inverse of the laser repetition rate. v_a is the sonic speed, as mentioned.

Figure 4 verifies the radiation spectra, as shown in the insets of Figs. 3(a) and 3(b) by comparing them with two theoretical calculations based on Eq. (2): one for the phased array in the far field ($r =$ infinity), and the other one with the actual experimental distance of detection ($r \approx 0.1$ m). For the radiation spectrum detected at 0° in Fig. 4(a), both theoretical and experimental results exhibit a spectrum peak of around 12.7 kHz with an FWHM of around 600 Hz. In this case, the far-field model does not deviate from the one calculated with the detection distance $r \approx 0.1$ m. However, in comparison, the radiation spectrum detected at 30° does not coincide well with the theoretical results: the experimentally measured peak frequency is 15.68 kHz as compared to 16.03 and 15.38 kHz from the two theoretical models and its corresponding FWHM is ~900 Hz as compared to 1.5 and 2 kHz. This difference is mainly caused by the scattered acoustic wave decaying into the far field. Hence, for the fixed moving velocity, there are only a limited number of scatters that can contribute to the radiation in the far field.

4. Discussion and Conclusion

Similar to photonic SPR with an undulator configuration, our SPR-like photoacoustic phased array can also be tailored for particular acoustic wave emission in terms of bandwidth, frequency, and emission angle by engineering microstructured gratings, i.e., metamaterials. In this manner, a compact acoustic wave source with dispersive spreading frequency emission

can be obtained, similar to an optical grating, which might be beneficial for some acoustic spectroscopy applications[33]. Meanwhile, acoustic SPR is not limited to free space; it is also applicable for bulk conditions, e.g., exciting phonons within layered materials[34]. For example, it has been proposed to generate terahertz waves using semiconductor superlattices by considering SPR-based phonon–photon interactions[35]. These photo-excited phonons have been well studied using ultrafast laser pulsed for their propagation and interaction[29,36]. We believe this acoustic analogy of the Smith–Purcell effect may finally open a new avenue in condensed matter, acoustics, and phononics.

In conclusion, we have demonstrated an SPR-like photoacoustic phased array based on laser-induced surface shock waves. The mechanisms of organizing such a related phase item in our photoacoustic case share a similarity to the original photonic SPR. As a result, the observed radiation spectrum in the far field can be well described by a universal theory working both for the photonic SPR and our acoustic one. We believe similar studies can be further extended to other physical systems like phonons in the solid-state system.

Acknowledgement

This work was supported by the National Natural Science Foundation of China (Nos. 92050113 and 11674228), the National Key Research and Development Program of China (Nos. 2016YFA0302500 and 2017YFA0303700), and the Shanghai MEC Scientific Innovation Program (No. E00075).

References

1. S. J. Smith and E. M. Purcell, "Visible light from localized surface charges moving across a grating," Phys. Rev. **92**, 1069 (1953).
2. G. Doucas, J. H. Mulvey, M. Omori, J. Walsh, and M. F. Kimmitt, "First observation of Smith-Purcell radiation from relativistic electrons," Phys. Rev. Lett. **69**, 1761 (1992).
3. M. J. Moran, "X-ray generation by the Smith-Purcell effect," Phys. Rev. Lett. **69**, 2523 (1992).
4. D. Li, M. Nakajima, M. Tani, J. Yang, H. Kitahara, M. Hashida, M. Asakawa, W. Liu, Y. Wei, and Z. Yang, "Terahertz radiation from combined metallic slit arrays," Sci. Rep. **9**, 6804 (2019).
5. D. A. G. Deacon, L. R. Elias, J. M. J. Madey, G. J. Ramian, H. A. Schwettman, and T. I. Smith, "First operation of a free-electron laser," Phys. Rev. Lett. **38**, 892 (1977).
6. V. Kumar and K.-J. Kim, "Analysis of Smith-Purcell free-electron lasers," Phys. Rev. E **73**, 026501 (2006).
7. E. Saldin, E. Schneidmiller, and M. V. Yurkov, *The Physics of Free Electron Lasers* (Springer Science & Business Media, 1999).
8. K.-J. Kim, "Characteristics of synchrotron radiation," AIP Conf. Proc. **184**, 565 (1989).
9. D. M. Asner, R. F. Bradley, L. de Viveiros, P. J. Doe, J. L. Fernandes, M. Fertl, E. C. Finn, J. A. Formaggio, D. Furse, A. M. Jones, J. N. Kofron, B. H. LaRoque, M. Leber, E. L. McBride, M. L. Miller, P. Mohanmurthy, B. Monreal, N. S. Oblath, R. G. H. Robertson, L. J. Rosenberg, G. Rybka, D. Rysewyk, M. G. Sternberg, J. R. Tedeschi, T. Thummler, B. A. VanDevender, and N. L. Woods, "Single-electron detection and spectroscopy via relativistic cyclotron radiation," Phys. Rev. Lett. **114**, 162501 (2015).
10. G. Adamo, K. F. MacDonald, Y. H. Fu, C. M. Wang, D. P. Tsai, F. J. García de Abajo, and N. I. Zheludev, "Light well: a tunable free-electron light source on a chip," Phys. Rev. Lett. **103**, 113901 (2009).
11. I. Kaminer, S. E. Kooi, R. Shiloh, B. Zhen, Y. Shen, J. J. López, R. Remez, S. A. Skirlo, Y. Yang, and J. D. Joannopoulos, "Spectrally and spatially resolved Smith-Purcell radiation in plasmonic crystals with short-range disorder," Phys. Rev. X **7**, 011003 (2017).
12. M. Henstridge, C. Pfeiffer, D. Wang, A. Boltasseva, V. M. Shalaev, A. Grbic, and R. Merlin, "Synchrotron radiation from an accelerating light pulse," Science **362**, 439 (2018).
13. Y. Ye, F. Liu, M. Wang, L. Tai, K. Cui, X. Feng, W. Zhang, and Y. Huang, "Deep-ultraviolet Smith–Purcell radiation," Optica **6**, 592 (2019).
14. P. M. Van den Berg, "Smith–Purcell radiation from a point charge moving parallel to a reflection grating," J. Opt. Soc. Am. **63**, 1588 (1973).
15. A. Hessel, J. Schmoys, and D. Y. Tseng, "Bragg-angle blazing of diffraction gratings," J. Opt. Soc. Am. **65**, 380 (1975).
16. A. Gover, P. Dvorkis, and U. Elisha, "Angular radiation pattern of Smith–Purcell radiation," J. Opt. Soc. Am. B **1**, 723 (1984).
17. I. Shih, W. W. Salisbury, D. L. Masters, and D. B. Chang, "Measurements of Smith–Purcell radiation," J. Opt. Soc. Am. B **7**, 345 (1990).
18. W. Ng, A. A. Walston, G. L. Tangonan, J. J. Lee, I. L. Newberg, and N. Bernstein, "The first demonstration of an optically steered microwave phased array antenna using true-time-delay," J. Light. Technol. **9**, 1124 (1991).
19. X. Xu, J. Wu, T. G. Nguyen, T. Moein, S. T. Chu, B. E. Little, R. Morandotti, A. Mitchell, and D. J. Moss, "Photonic microwave true time delays for phased array antennas using a 49 GHz FSR integrated optical micro-comb source [Invited]," Photonics Res. **6**, B30 (2018).
20. A. Derode, P. Roux, and M. Fink, "Robust acoustic time reversal with high-order multiple scattering," Phys. Rev. Lett. **75**, 4206 (1995).
21. M. H. Noroy, D. Royer, and M. Fink, "The laser-generated ultrasonic phased array: analysis and experiments," J. Acoust. Soc. Am. **94**, 1934 (1993).
22. R. K. Ing, F. Gires, and M. Fink, "Focusing and beamsteering of laser generated ultrasound," Ultrason. Symp. Proc. **1**, 539 (1989).
23. P. F. McManamon, T. A. Dorschner, D. L. Corkum, L. J. Friedman, D. S. Hobbs, M. Holz, S. Liberman, H. Q. Nguyen, D. P. Resler, R. C. Sharp, and E. A. Watson, "Optical phased array technology," Proc. IEEE **84**, 268 (1996).
24. J. Sun, E. Timurdogan, A. Yaacobi, E. S. Hosseini, and M. R. Watts, "Large-scale nanophotonic phased array," Nature **493**, 195 (2013).
25. V. L. Ginzburg, "Radiation by uniformly moving sources (Vavilov–Cherenkov effect, transition radiation, and other phenomena)," Phys. Usp. **39**, 973 (1996).
26. N. Dahan, Y. Gorodetski, K. Frischwasser, V. Kleiner, and E. Hasman, "Geometric Doppler effect: spin-split dispersion of thermal radiation," Phys. Rev. Lett. **105**, 136402 (2010).
27. M. P. Silverman and G. M. Cushman, "Voice of the dragon: the rotating corrugated resonator," Eur. J. Phys. **10**, 298 (1989).
28. T. E. Stevens, J. K. Wahlstrand, J. Kuhl, and R. Merlin, "Cherenkov radiation at speeds below the light threshold: phonon-assisted phase matching," Science **291**, 627 (2001).
29. T. Feurer, J. C. Vaughan, and K. A. Nelson, "Spatiotemporal coherent control of lattice vibrational waves," Science **299**, 374 (2003).
30. J. K. Wahlstrand and R. Merlin, "Cherenkov radiation emitted by ultrafast laser pulses and the generation of coherent polaritons," Phys. Rev. B **68**, 54301 (2003).
31. A. M. Azzeer, A. S. Al-Dwayyan, M. S. Al-Salhi, A. M. Kamal, and M. A. Harith, "Optical probing of laser-induced shock waves in air," Appl. Phys. B **63**, 307 (1996).
32. D. T. Blackstock, *Fundamentals of Physical Acoustics* (Wiley, 2000).
33. H. Kawashima, M. M. Wefers, and K. A. Nelson, "Femtosecond pulse shaping, multiple-pulse spectroscopy, and optical control," Annu. Rev. Phys. Chem. **46**, 627 (1995).
34. Y. Zhang, C. Hu, B. Lyu, H. Li, Z. Ying, L. Wang, A. Deng, X. Luo, Q. Gao, and J. Chen, "Tunable Cherenkov radiation of phonon polaritons in silver nanowire/hexagonal boron nitride heterostructures," Nano Lett. **20**, 2770 (2020).
35. A. A. Maznev, K. J. Manke, K.-H. Lin, K. A. Nelson, C.-K. Sun, and J.-I. Chyi, "Broadband terahertz ultrasonic transducer based on a laser-driven piezoelectric semiconductor superlattice," Ultrasonics **52**, 1 (2012).
36. Y. X. Yan, E. B. Gamble, and K. A. Nelson, "Impulsive stimulated scattering: general importance in femtosecond laser pulse interactions with matter, and spectroscopic applications," J. Chem. Phys. **83**, 5391 (1985).